

05
Study of the radial distribution of magnetic permeability over the cross-section of amorphous soft magnetic wire $\text{Co}_{66}\text{Fe}_4\text{Nb}_{2.5}\text{Si}_{12.5}\text{B}_{15}$ using magnetoimpedance tomography

© D.A. Bukreev, I.M. Matsyuk, M.S. Derevyanko, A.V. Shapovalova, A.A. Moiseev, A.V. Semirov

Irkutsk State University,
664003 Irkutsk, Russia
e-mail: rezervimm@gmail.com

Received October 7, 2025

Revised December 10, 2025

Accepted December 15, 2025

The results of a study on the radial distribution of magnetic permeability across the cross-section of an amorphous soft magnetic wire made of the $\text{Co}_{66}\text{Fe}_4\text{Nb}_{2.5}\text{Si}_{12.5}\text{B}_{15}$ alloy in the magnetic field range from 0 to 12.3 kA/m are presented. The results were obtained using the magnetoimpedance tomography method, taking into account the external inductance of the wire. It was found that for the outer region of the wire with a thickness of 2.5 μm , in the absence of an external magnetic field, the magnetic permeability values do not exceed 100, while the magnetic permeability of the inner region reaches 13 500. The nature of the changes in the magnetic permeability of the outer and inner regions in an external magnetic field is also different.

Keywords: magnetoimpedance tomography, amorphous wires, computer simulation, magnetoimpedance, magnetic permeability.

DOI: 10.61011/TP.2026.04.63265.280-25

Introduction

Soft magnetic amorphous wires produced by fast quenching from a melt [1] are actively used in modern electronics. For example, they are applied as sensitive elements of detectors of low magnetic fields [2–4]. It is possible due to an effect of magnetoimpedance (MI), which consists of a dependence of complex electrical resistance of a conductor to alternating current (impedance) on strength of an external magnetic field [5,6]. In the amorphous wires based on cobalt, magnetoimpedance can have values exceeding 100 % even in the low magnetic fields [7,8].

The amorphous wires produced by fast quenching from the melt are characterized by a complex radial distribution of internal mechanical stresses that occur during fabrication [9,10]. Since their magnetic anisotropy has a generally magnetic elastic nature, it results in the inhomogeneous distribution of the magnetic properties.

In case of wires in a glass shell, the radial distribution is significantly affected by a glass coating that affects the value and distribution of internal stresses [11].

The radial distribution of circular magnetic permeability of the wire can be restored using Magnetoimpedance Tomography (MIT). This method is based on analysis of MI frequency dependences and well proven in case of amorphous fast-quenched and composite wires [12]. The mentioned study compares the experimental frequency dependences with dependences calculated using Finite Element Method. At the same time, a conductor model is divided into several layers and inside each of them the magnetic and electric parameters are assumed to be unchanged. It is obvious that the more layers, the more accurately the

restored distribution of magnetic permeability corresponds to a real one. This MIT implementation was considered theoretically as well in the study [13]. At the same time, frequency dispersion of magnetic permeability was also taken into account. Previously, the MIT implementation of the amorphous microwires, which is based on using an expression of impedance of a homogeneous conductor of cylindrical geometry [14,15], was proposed as well. We note that application of this MIT implementation is limited when the distribution of magnetic permeability across a wire cross-section is highly inhomogeneous.

The inhomogeneous distribution of the magnetic properties across the cross-section is also found in case of amorphous soft magnetic tapes [16], which can also be studied by the MIT method.

The present study provides the MIT results for the amorphous soft magnetic wires $\text{Co}_{66}\text{Fe}_4\text{Nb}_{2.5}\text{Si}_{12.5}\text{B}_{15}$. MIT was used to restore the distributions of magnetic permeability across the wire cross-section in the magnetic fields from 0 to 12.3 kA/m.

1. Materials and methods

Samples for an experimental study were segments of the amorphous soft magnetic wire $\text{Co}_{66}\text{Fe}_4\text{Nb}_{2.5}\text{Si}_{12.5}\text{B}_{15}$ of the 90 μm radius. A magnetostriction constant is weak and positive and it is below 10^{-7} . The magnetic hysteresis loops were obtained by an induction method. A remagnetization magnetic field oriented along the sample length varied with the 1 kHz frequency and its amplitude was 1200 A/m. The magnetic hysteresis loops obtained on the different-length

samples were taken to determine a value of saturation induction $B_s \approx 0.4$ T as well as the dependence of the ratio B_r/B_s (B_r residual induction) on the wire length l (Fig. 1). When the wire length decreases from 100 to 80 mm, the ratio B_r/B_s remains almost unchanged. When $l < 80$ mm, reduction of the wire length results in a quite fast drop of B_r/B_s , which is related to an increase of influence of demagnetizing fields from its face ends [17]. For this reason, the studies were performed on the samples of the 100 mm length.

Impedance Z was measured by means of a measuring unit described in the study [18]. Impedance was measured along a portion of the 24 mm length, which was in the middle of the sample. The alternating current of an rms value of 1 mA was flowing along the sample length, and its frequency f varied within the range from 0.01 to 80 MHz. The external magnetic field H was also oriented along the sample length. Its maximum strength H_{max} reached ± 12.3 kA/m. The measurement results were presented as dependences $Z(f)/R_{dc}$, where R_{dc} is direct-current resistance.

Magnetic impedance was calculated by the formula

$$\frac{\Delta Z}{Z(H)} = \frac{Z(H) - Z(H_{max})}{Z(H_{max})} \cdot 100\%, \quad (1)$$

where $Z(H)$ is a scalar impedance measured in the magnetic field of strength of H , $Z(H_{max})$ is a scalar impedance measured in the magnetic field of strength of H_{max} . Maximum relative errors of measurement of impedance Z and strength of the external magnetic field H did not exceed 3% and 2%, respectively.

The dependences $Z(f)/R_{dc}$ designed to be a base for MIT [12] were simulated by the finite element method by means of the Comsol Multiphysics software package (the license №. 9602434). The wire model was divided into $n = 7$ coaxial cylindrical domains of the radii r_i , $i = 1, 2, \dots, n$. Each cylindrical layer obtained was assigned with a value of magnetic permeability μ_i .

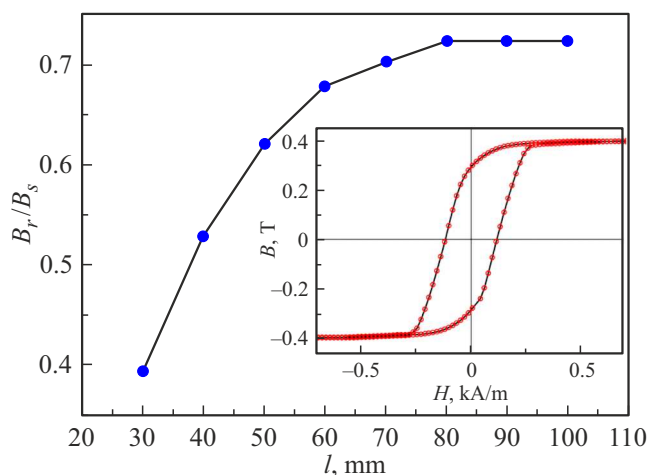


Figure 1. Dependence of the ratio B_r/B_s on the length of the amorphous soft magnetic wire $\text{Co}_{66}\text{Fe}_4\text{Nb}_{2.5}\text{Si}_{12.5}\text{B}_{15}$. The insert includes a loop of magnetic hysteresis of the wire $\text{Co}_{66}\text{Fe}_4\text{Nb}_{2.5}\text{Si}_{12.5}\text{B}_{15}$ of the 100 mm length.

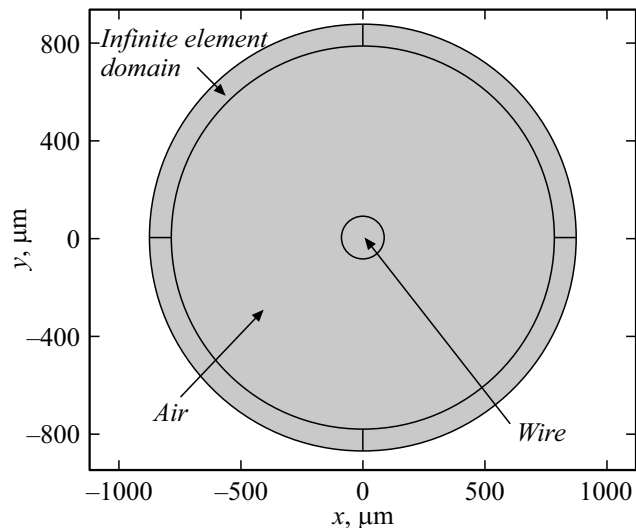


Figure 2. Geometry of the wire model Wire and its surrounding domains Air and Infinite element domain for calculation in Comsol Multiphysics.

In order to take into account external inductance of the wire, the cylindrical domain Air of the radius $10r_n$ was simulated around it. Magnetic permeability and electrical conductance of this domain were 1 and 0, respectively. Closure of power lines of the magnetic field outside the domain Air was simulated by means of a tool Infinite element domain (Fig. 2).

Simulation done at various combinations of μ_i and r_i resulted in obtaining the dependences $Z(f)/R_{dc}$. In doing so, the values of the frequencies were the same as in the experiment. The values of r_6 and r_5 were varied with a step of $0.1 \mu\text{m}$ around 89 and $87 \mu\text{m}$, respectively. The radii of the deeper layers were changed with a step of $5 \mu\text{m}$. Magnetic permeabilities of all the layers μ_i were varied within the limits from 1 to 14 000. Conductivity of all the layers was assumed to be 624 kS/m .

In an array of the simulated dependences $Z(f)/R_{dc}$, we found the dependence that had the least deviation from the experimental dependence (Fig. 3,4). A combination of μ_i and r_i , at which this dependence was simulated, was assumed to be reflecting a real distribution of magnetic permeability across the cross-section of the wire. We note that the best results were provided by the combination r_i that is given in Table.

MITs of the amorphous soft magnetic wires of the same composition as in the present study were performed previously as well [19]. But the wire model with the smaller number of the layers was used — $n = 5$. In doing so, external inductance was not taken into account. As a result, the deviation of the simulated and experimental dependences $Z(f)/R_{dc}$ reached 6% (Fig. 3). When $n = 7$ and external inductance is taken into account, the maximum deviation does not exceed 1% within the entire studied frequency range and the field interval (Fig. 4).

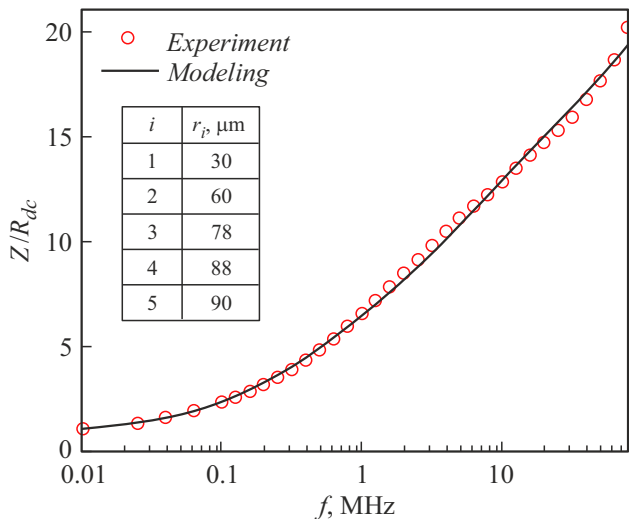


Figure 3. Experimental and simulated dependences $Z(f)/R_{dc}$ when $n = 5$. The value of $H = 0$ kA/m.

We note that during simulation the present study took into account neither dispersion of magnetic permeability nor a contribution to magnetic permeability by the wire, which is related to motion of domain boundaries. These issues can be discussed in future studies.

2. Results and discussion

The MIT results of the wire in the different-strength fields are shown in Fig. 5 and 6.

According to the MIT results, the distribution of magnetic permeability across the cross-section of the wire is highly inhomogeneous. Thus, in the zero external magnetic field magnetic permeability varies from 100 (the external layer) to 13 500 (Fig. 5). In the magnetic field of about 12 kA/m, the value of magnetic permeabilities varies from 1 to 350

Values of r in the model used

Layer number i	External radius of the layer $r_i, \mu\text{m}$
1	40
2	50
3	65
4	85
5	87.5
6	88.4
7	90

(Fig. 6). In the low magnetic fields, the distribution $\mu(r)$ outlines two layers (the 2-nd and the 5-th), whose permeabilities are much higher than those of the adjacent layers (Fig. 5). For the second layer, it seems to be related to a minimum on the radial distribution of internal quenching stresses and, respectively, to a minimum of magnetic elastic anisotropy. Presence of the minimum of magnetic elastic anisotropy follows from the results of theoretical consideration of the radial distribution of internal quenching stresses in the amorphous fast-quenched wires [9]. The high value of magnetic permeability of the fifth layer is probably due to a transition from a circularly-magnetized surface layer to an axially-magnetized main volume of the wire. We note that existibility of a thin transitional layer with high magnetic permeability and its influence on magnetic impedance was theoretically discussed previously in the study [20].

Let us consider changes of magnetic permeabilities of the wire layers in the external magnetic field. As can be seen from Fig. 7, magnetic permeabilities of the internal layers of the wire (the layers 1–5) decrease with an increase of strength of the external magnetic field (Fig. 7, a). Magnetic

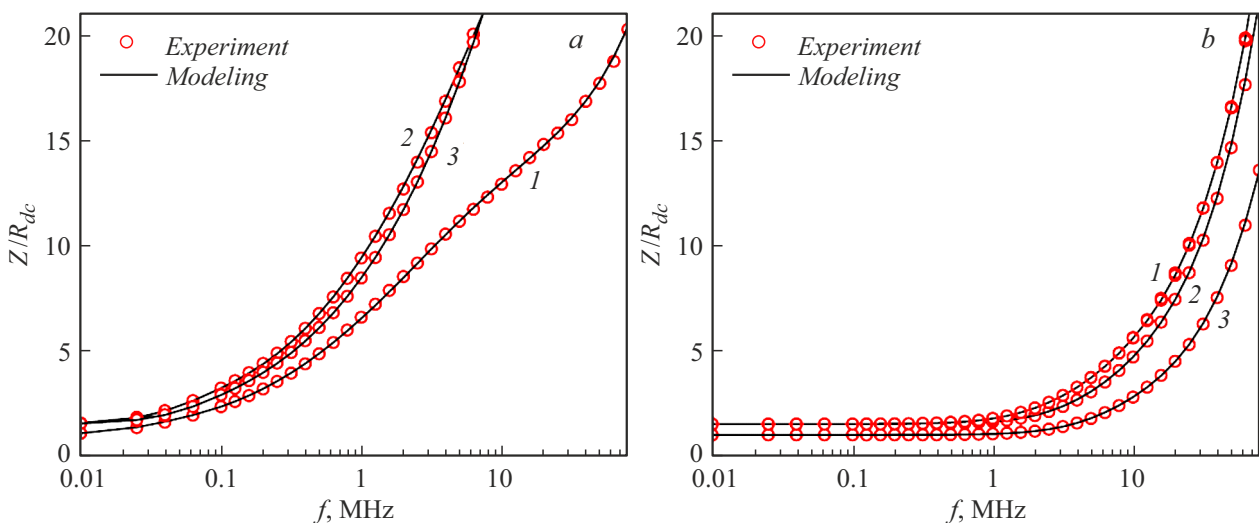


Figure 4. Experimental and simulated dependences $Z(f)/R_{dc}$ when $n = 7$. The values of H : a — 1 — 0, 2 — 0.019, 3 — 0.038 kA/m; b — 1 — 6.6, 2 — 9.4, 3 — 12.3 kA/m.

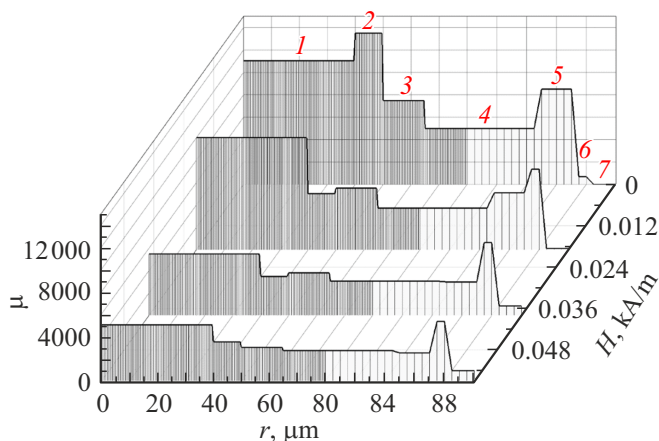


Figure 5. Radial distribution of circular magnetic permeability of the wire $\text{Co}_{66}\text{Fe}_4\text{Nb}_{2.5}\text{Si}_{12.5}\text{B}_{15}$ in the magnetic fields of strength 0, 0.019, 0.038, 0.057 kA/m, which is restored by means of the MIT method.

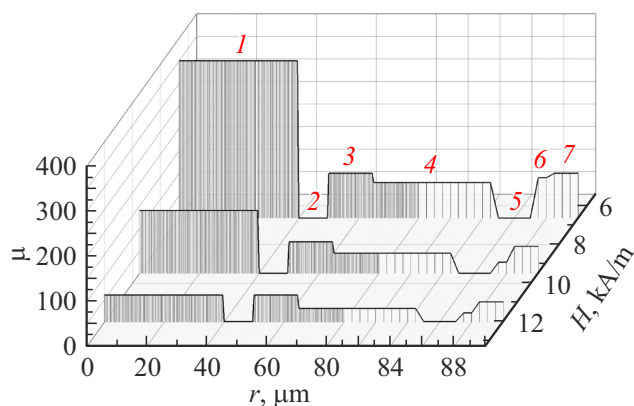


Figure 6. Radial distribution of circular magnetic permeability of the wire $\text{Co}_{66}\text{Fe}_4\text{Nb}_{2.5}\text{Si}_{12.5}\text{B}_{15}$ in the magnetic fields of strength 6.6, 9.4, 12.3 kA/m, which is restored by means of the MIT method.

permeabilities of the external layers of the wire (Fig. 7, *b*) with the increase of H behave differently: μ_i first increase and then decrease. In doing so, magnetic permeability of the seventh layer reaches a maximum in the field of 57 A/m, so does magnetic permeability of the sixth layer in the field of about 19 A/m.

A nature of variation of magnetic permeability in the external magnetic field makes it possible to judge specific features of magnetic anisotropy. The dependence $\mu(H)$, which monotonically decreases with an increase of strength of the axial external magnetic field, indicates predominantly axial magnetic anisotropy. In turn, presence of an increasing portion on the dependence $\mu(H)$ within the low-field range indicates predominance of circular magnetic anisotropy. Thus, it can be concluded based thereon that the wire's thin external layer of the 2.5 μm thickness has predominantly circular anisotropy,

while the remaining volume of the wire has predominantly axial anisotropy. The obtained conclusion agrees with earlier results of studies of the wire of this composition [19].

Below we address the MI dependences on strength of the external magnetic field H , which are obtained at the different frequencies of alternating current (Fig. 8). At the alternating current's frequencies below 3 MHz, MI monotonically decreases with an increase of strength of the magnetic field — the dependences $\Delta Z/Z(H)$ are shaped as „one peak“ (Fig. 8, *a*). With the increase of the alternating current's frequency, as a depth of a skin layer decreases and the contribution to the MI response from the surface domains increases, the low-field dependences $\Delta Z/Z(H)$ exhibit an increasing portion, i.e. they are shaped as „two peaks“. As it is known, the nature of MI variation in the external magnetic field is related to the respective nature of variation of magnetic permeability [20,21]. Thus, taking into account the above-discussed MIT results, it can be concluded that presence of the increasing portion on the dependences $\Delta Z/Z(H)$ is related to the thin wire's surface layer of the 2.5 μm thickness. The dependences $\Delta Z/Z(H)$, which have the increasing portion in the low fields, are the most interesting for practical applications, since exactly at this portion the highest sensitivity of MI to the external magnetic field is usually achieved.

Conclusion

The MIT method was taken to study the radial distribution of magnetic permeability of the amorphous soft magnetic wire $\text{Co}_{66}\text{Fe}_4\text{Nb}_{2.5}\text{Si}_{12.5}\text{B}_{15}$ of the 90 μm radius within the range of strengths of the external axial magnetic field from 0 to 12.3 kA/m. MIT included use of the seven-layer model and taking into account external inductance of the wire.

Without the external magnetic field, a subsurface domain of the thickness of about 2.5 μm has permeability that does not exceed 100, while in the internal domain of the wire it reaches the value of about 13 500. The distribution of magnetic permeability inside each of the domains is highly inhomogeneous. The behavior of magnetic permeabilities of the subsurface and the internal domains in the external magnetic field is also different: the surface layers demonstrated presence of maximums of magnetic permeability at the low fields (19 and 57 A/m) due to predominance of circular magnetic anisotropy. The internal layers demonstrate monotonic reduction of magnetic permeability with the increase of strength of the magnetic field, thereby indicating predominance of axial magnetic anisotropy. This inhomogeneous magnetic structure is caused by the complex distribution of internal quenching stresses that originate during production of these amorphous wires.

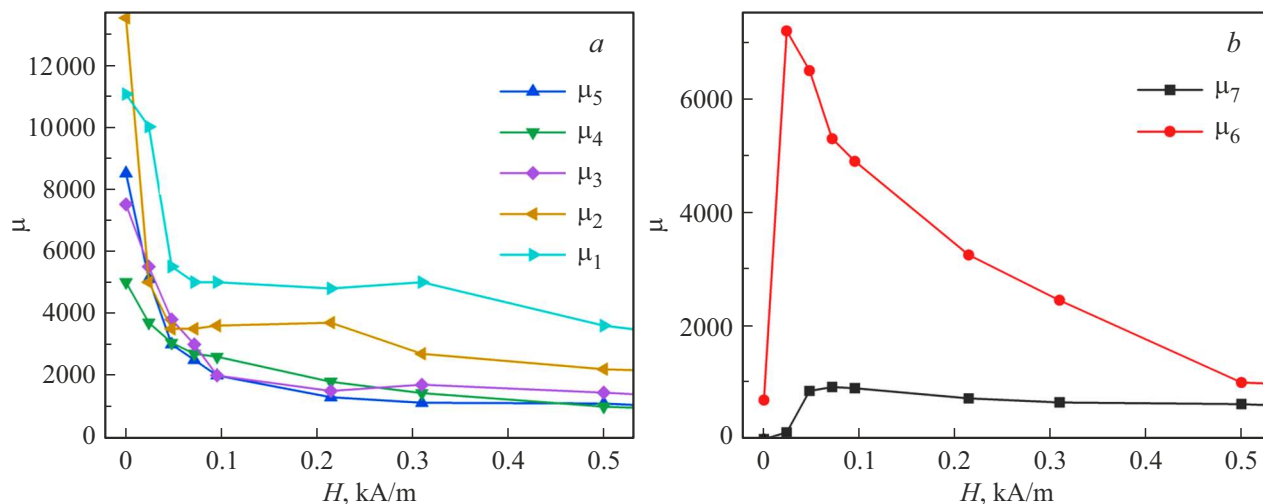


Figure 7. Field dependences of circular magnetic permeabilities of the wire $\text{Co}_{66}\text{Fe}_4\text{Nb}_{2.5}\text{Si}_{12.5}\text{B}_{15}$, which are restored by means of the MIT method: μ_1 – μ_5 (a); μ_6 and μ_7 (b).

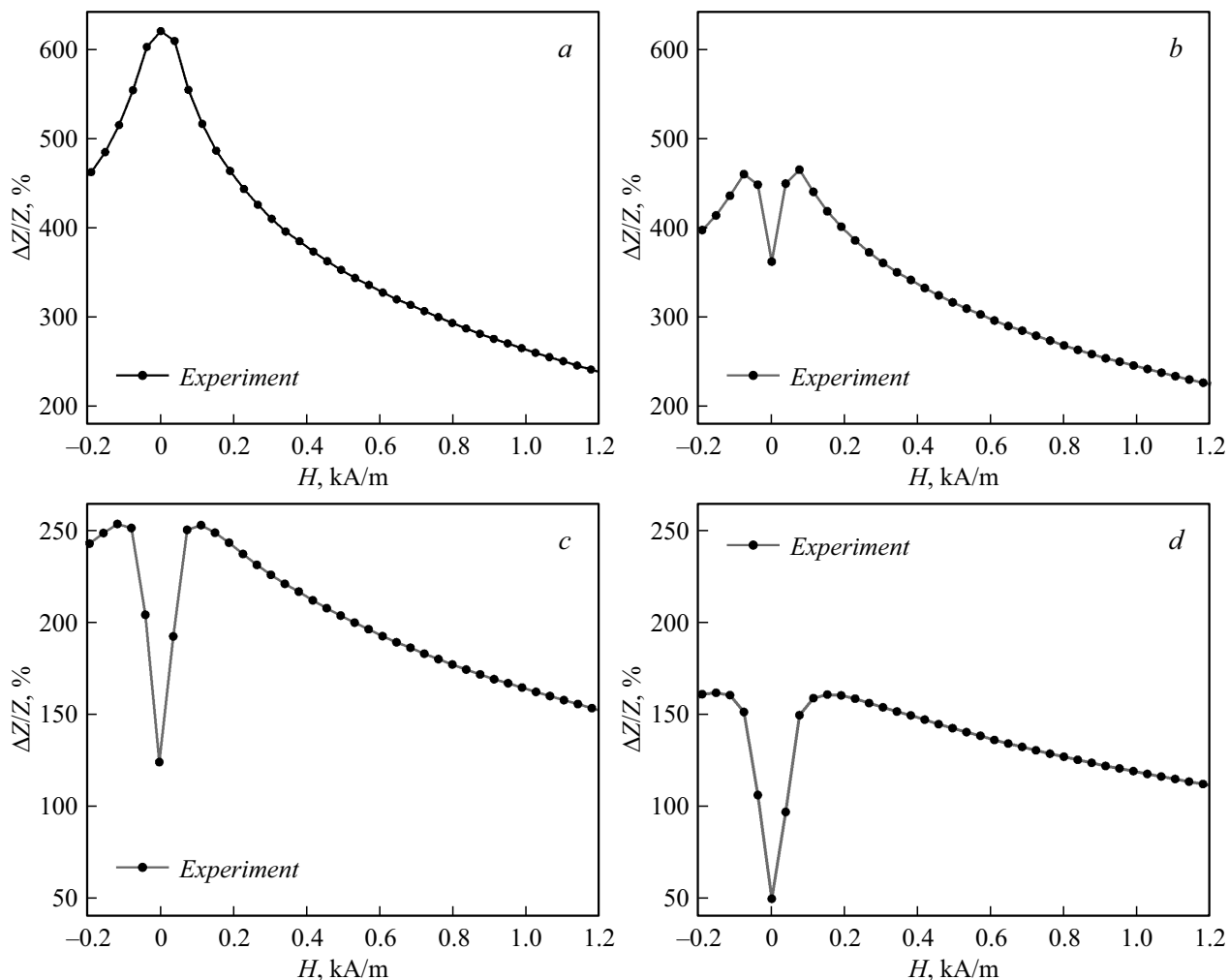


Figure 8. Dependences of the MI effect on strength of the magnetic field H , which are obtained at the following values of the alternating current frequencies: a – 2, b – 10, c – 40, d – 80 MHz.

Funding

The studies were performed using a grant from the Russian Science Foundation № 22-22-00709, <https://rscf.ru/project/22-22-00709/>.

Conflict of interest

The authors declare that they have no conflict of interest.

References

- [1] T. Masumoto, I. Ohnaka, A. Inoue, M. Hagiwara. *Scripta Metallurgica*, **15**, 293 (1981). DOI: 10.1016/0036-9748(81)90347-1
- [2] V. Fal-Miyar, A. Kumar, S. Mohapatra, S. Shirley, N.A. Frey, J.M. Barandiarand, G.V. Kurlyandskaya. *Appl. Phys. Lett.*, **91**, 143902 (2007).
- [3] K. Fodil, M. Denoual, C. Dolabdjian, A. Treizebre, V. Senez. *Appl. Phys. Lett.*, **108**, 173701 (2016). DOI: 10.1063/1.4948286
- [4] J. Chen, J. Li, Y. Li, Y. Chen, L. Xu. *Sensors*, **18**, 732 (2018). DOI: 10.3390/s18030732
- [5] R.S. Beach, A.E. Berkowitz. *Appl. Phys. Lett.*, **64**, 3652 (1994). DOI: 10.1063/1.111170
- [6] L.V. Panina, K. Mohri. *Appl. Phys. Lett.*, **65**, 1189 (1994). DOI: 10.1063/1.112104
- [7] K. Mohri, T. Uchiyama, L.V. Panina, M. Yamamoto, K. Bushida. *J. Sensors*, **215**, 718069 (2015). DOI: 10.1155/2015/718069
- [8] K. Nesteruk, M. Kuzminski, H.K. Lachowicz. *Sensors Transducers Magazine (S & Te-Digest)*, **65** (3), 515 (2006).
- [9] A.S. Antonov, V.T. Borisov, O.V. Borisov, V.A. Pozdnyakov, A.F. Prokoshin, N.A. Usov. *Phys. D: Appl. Phys.*, **32**, 1788 (1999). DOI: 10.1088/0022-3727/32/15/305
- [10] V. Madurga, A. Hernando. *J. Phys.: Condens. Matter*, **2**, 2127 (1990).
- [11] O.I. Aksenov, A.A. Fuks, A.S. Aronin. *J. Alloys Compounds*, **836**, 155472 (2020). DOI: 10.1016/j.jallcom.2020.155472
- [12] D.A. Bukreev, M.S. Derevyanko, A.A. Moiseev, A.V. Svalov, A.V. Semirov. *Sensors*, **22**, 9512 (2022). DOI: 10.3390/s22239512
- [13] N.A. Buznikov, G.V. Kurlyandskaya. *Sensors*, **24**, 3669 (2024). DOI: 10.3390/s24113669
- [14] Y.A. Alekhina, V. Kolesnikova, A.S. Komlev, M. Khajrullin, L.A. Makarova, V.V. Rodionova, N.S. Perov. *J. Magn. Magn. Mater.*, **537**, 168155 (2021). DOI: 10.1016/j.jmmm.2021.168155
- [15] I. Alekhina, V. Kolesnikova, V. Rodionov, N. Andreev, L.V. Panina, L. Rodionova, N. Perov. *Nanomaterials*, **11** (2), 274 (2021). DOI: 10.3390/nano11020274
- [16] N.A. Skulkina, E.S. Nekrasova. *Fizika metallov i metallovedenie*, **124** (8), 703 (2023) (in Russian). DOI: 10.31857/S0015323023600648
- [17] D.A. Bukreev, M.S. Derevyanko, A.A. Moiseev, A.V. Semirov. *Fizika metallov i metallovedenie*, **124** (8), 710 (2023) (in Russian). DOI: 10.31857/s0015323023600673
- [18] D.A. Bukreev, M.S. Derevyanko, A.A. Moiseev, A.V. Semirov, P.A. Savin, G.V. Kurlyandskaya. *Materials*, **13**, 3216 (2020). DOI: 10.3390/ma13143216
- [19] A.A. Moiseev, D.A. Bukreev, M.S. Derevyanko, A.V. Semirov. *Tech. Phys.*, **69** (1), 66 (2024). DOI: 10.61011/JTF.2024.01.56903.189-23
- [20] D.X. Chen, L. Pascual, E. Fraga, M. Vazquez, A. Hernando. *J. Magn. Magn. Mater.*, **202**, 2 (1999). DOI: 10.1016/S0304-8853(99)00420-5
- [21] N.A. Usov, A.S. Antonov, A.N. Lagarkov. *J. Magn. Magn. Mater.*, **185**, 159 (1998). DOI: 10.1016/S0304-8853(97)01148-7

Translated by M. Shevelev